Discoveries in Agriculture and Food Sciences - Vol. 11, No. 3
Publication Date: June 25, 2023
DOI:10.14738/dafs.113.14904.
Yamani, H. A., Othman, A., & Gashgari, R. (2023). Phytochemical Analysis and Nanoparticles-Based Bioactivity Screening of Five Medicinal Plant Extracts. Discoveries in Agriculture and Food Sciences, 11(3). 63-76.

Phytochemical Analysis and Nanoparticles-Based Bioactivity Screening of Five Medicinal Plant Extracts

Hanaa Abbas Yamani
Department of Biology, College of Science,
University of Jeddah, Jeddah, Saudi Arabia

Abrar Othman
Department of Biology, College of Science,
University of Jeddah, Jeddah, Saudi Arabia

Rukaia Gashgari
Department of Biology, College of Science,
University of Jeddah, Jeddah, Saudi Arabia

ABSTRACT

This study investigated the presence of bioactive phytochemical compounds in five medicinal plant extracts using nanoparticles. Silver nanoparticles were synthesized using aqueous extracts of five medicinal plants including Juniperus excelsa, Moringa oleifera, Prosopis juliflora, Pithecellobium dulce, and Eucalyptus globulus. The plants were randomly collected from the cities of Jeddah and Taif, Kingdom of Saudi Arabia. The total polyphenolic contents of plant extracts were determined through GCMS and HPLC. The nanoparticle synthesizing efficiency of plant extracts was also examined and XRD, UV-Vis spectroscopy, and zeta potential measurements were performed for nanoparticle characterization. The nanoparticle formation rate was assessed through UV-Vis spectroscopy. The results confirmed the antimicrobial efficacy of examined plant extracts and suggested their potential application for infectious disease treatments.

Keywords: Silver Nanoparticles, Green Synthesis, Antimicrobial activity, Plant extract, GCMS, HPLC.

INTRODUCTION

Antimicrobial plant extracts can serve as effective natural alternatives to synthetic agents [1]. World Health Organization (WHO) reports reveal that active compounds-containing plant extracts are frequently used in folk medicine for traditional therapies of a large global population (80%). More than 50% of modern medicines have originated from natural products [2]. Phytochemical elements such as tannins, vitamins (A, E, K, and C), pigments, carotenoids, alkaloids, terpenoids, polyphenols, flavonoids, saponins, minerals, and enzymes are known to exert antioxidant and antimicrobial activities [3]. Antimicrobial characteristics of various plant compounds have been explored, which are produced during secondary plant metabolism [4].

Multidrug-resistant strains are rising alarmingly that pose serious threats to humans [5]. Antibiotic resistance is mainly associated with the complex interaction of different factors such

as reduced permeability, drug inactivation, and target alteration leading to the evolution and plasmid-based expansion in resistance mechanisms [6]. Extensive and overused antibiotic therapies are the primary source of rising bacterial resistance. Nanomedicine has significantly emerged during the last decade because of the successful nanoconjugate outcomes against pathogens [7].

Multiple physical, biological, and chemical approaches have been devised for nanoparticle generation. The applications of silver nanoparticles (AgNPs) in biomedical treatments are significantly increasing [8]. Biological techniques are mainly employed to synthesize AgNPs, which involve plant materials, microorganisms, enzymes, and proteins. These materials are cost-effective, biocompatible, and eco-friendly facilitating large-scale nanoparticle synthesis [9, 10]. Plant-mediated green nanoparticle synthesis is an efficient strategy with immense applicability in modern medicine [11, 12]. Plant extracts perform as stabilizing and reducing agents during nanoparticle synthesis [13]. Medicinal plants generate several secondary metabolites possessing unique biological potential, particularly antimicrobial properties. Therefore, this study elaborated on the phytochemical properties of five medicinal plant extracts and their nanoparticle synthesis potential.

MATERIALS AND METHODS

Plant Samples

Fresh leaves of five medicinal plants (*J. excelsa*, *M. oleifera*, *P. juliflora*, *P. dulce,* and *E. globulus*) were randomly collected from the cities of Jeddah and Taif, Kingdom of Saudi Arabia from May 2017 to May 2018. The families of selected plants are enlisted in Table 1.

Table (1). Medicinal plants used in this study.

Scientific Name	Family	Common Name	Collection Site
Juniperus excelsa	Cupressaceae	Greek juniper	Taif
Moringa olefeira	Moringaceae	Moringa	Jeddah
Prosopis juliflora	Leguminosae	Mesquite	Jeddah
Pithecellobium dulce	Fabaceae	Tamarind	Jeddah
Eucalyptus globulus	Myrtaceae	Tasmanian bluegum or Southern blue gum	Taif

Plant Extract Preparation

Fresh leaves of *J. excelsa, M. oleifera, P. juliflora*, *P. dulce,* and *E. globulus* were multiple times rinsed with tap water followed by distilled water. The rinsed leaves were spread, air-dried, and grounded in an electrical mill. The powder of dried plants (10g) was added to 100 ml of ethanol (99.8%) in a conical flask that was plugged using sterile cotton. The samples were placed at 37°C in a shaker for 24 hours followed by 24 hours at room temperature. A muslin cloth followed by Whatman filter paper no. 1 was used to filter the extracts. The filtrates were dried at room temperature under reduced pressure. Finally, the extracts were dissolved in Dimethyl sulfoxide (DMSO) (0.25%).

Phytochemical Analysis

Sample powder (250 mg) was transferred to a methanol-containing clean test tube and mixed. The mixture was vortexed (30 sec), sonicated (10 min), and centrifuged (5000 rpm) for 10 min. Then, the mixture was filtered through a Nylon syringe filter membrane (0.2µ) and divided into two equal portions (1.5 ml each) in separate test tubes.

HPLC-DAD Analysis

The sample was prepared to calculate the amount of non-conjugated phenolic compounds including known flavanols. Briefly, the sample extract (1.5 mL) was placed in a glass test tube (15 ml) and dried using a gentle nitrogen gas stream at 50°C. Samples were reconstituted in methanol (100 µL), mixed with 100 µL of IS solution (Antipyrine 200 ng/µL), and vortexed (20 sec). 5 µL out of a total reaction volume of 1 mL was injected for analysis using a Pasteur pipette. A volume of sample extract (1.5 mL) was dried through evaporation in a test tube (15 mL) using nitrogen gas at 50°C. Dried residues were mixed with water (1.5 mL), hydrochloric acid solution (10M, 200 µL), and boiled for 1 h at 95°C over a hot thermostatic plate. Then, the mixture was cooled to room temperature, mixed with the ammonia solution (15M, 100 µL), and extracted using Chromabond® Solid Phase Extraction column (C18 ec, 3 mL/500 mg). The SPE column (C18 500 mg/3 mL) was conditioned with MeOH (5 mL) followed by elution with water (5 mL). The sample solution extract (1.8 mL) was added to the SPE column and allowed its slow flow through the extraction column (60 drops/min) by closing the tap. Then, the column was washed with water (5 mL), and residual water was expelled using nitrogen gas. The column was transferred to a clean test tube containing 100 µL of IS solution (Antipyrine 200 ng/µL), and adsorbed substances were eluted with MeOH (5 mL). The eluant was dried at 50°C using nitrogen gas, reconstituted in MeOH (200 µL), and 5 µL was injected for HPLC-DAD analysis. The amount of total phenolic compounds including flavanol was calculated whereas unknown flavonoids were mostly hydrolyzed to quercetin.

Gas Chromatography-Mass Spectrometry Conditions (GCMS)

Clarus 500 GC-MS (Perkin Elmer, Shelton, CT, USA) containing TurboMass controller/integrator software (5.4.2.1617) was used for the sample analyses. An Optima® 1 GC capillary column, Crossbond® 100% dimethyl polysiloxane (30-meter × 0.25 mmID × 0.25 µm df), (Macherey-Nagel, GMBH, Duren, Germany) was used. Helium (purity 99.9999%) gas served as the carrier at a flow rate of 0.90 ml/min. The source (EI+) temperature was 230˚C whereas 280˚C was the temperature of the GC inlet line. It had an electron energy of 70 eV and a trap emission of 100 v. The oven conditions were adjusted at an initial temperature of 60°C (hold for 5 min), raised to 80˚C (1˚C/min and hold for 2.0 min), and increased to 280˚C (5˚C/min and hold for 5.0 min). The injection volume was 1.0 µL whereas the split ratio was 60:1. Samples were assessed at a total MS scan from 40 to 500 m/z (500 scan/sec). The eluted compounds were characterized using NIST 2008.

Sample Preparation:

To prepare the samples, plant powder (500 mg) was transferred to a test tube (15 mL), and methanol (2 mL) was added and mixed. The solution was further vortexed (2 min), sonicated (5 min), and filtered through a nylon membrane (0.22 µm). A portion of this extract was added to the autosampler vial, and 1 µL was injected for GC-MS analysis. GC/MS presented characteristic peaks corresponding to the volatile materials without derivatization. MSTFA was

used for derivatizing the samples to obtain Trimethylsilylated derivatives, which were scanned with an EI-MS detector.

AgNPs Biosynthesis

$AgNO_3$ (1 mM, 50 mL) aqueous solution was mixed with an equal volume of aqueous plant extract and incubated at room temperature until the formation of a brownish color, which indicated AgNPs synthesis. AgNPs' green synthesis in colloidal solution was confirmed using a UV-visible spectrophotometer (PerkinElmer, USA) whereas distilled water served as the reference. The excessive Ag^+ ions were removed by centrifuging the AgNPs followed by washing with Milli-Q water.

Physicochemical Characterization of AgNPs

AgNPs were examined using field emission scanning microscopy/Energy dispersive X-ray (FESEM/EDX, (JSM-6701F, USA) to assess their surface morphology and chemical properties. Nanoparticles' surface functional groups were determined using Fourier-transformed infrared spectroscopy (FT-IR, Perkin Elmer, USA) through vibrational frequency alterations in the functional groups. X-ray diffraction (XRD) analysis of AgNPs was performed on an XRD instrument (Bruker axs System, D8, Germany) with a scanning range of 10˚ and 90˚. Nanoparticles' surface area was assessed by adopting the method of Brunauer-Emmett-Teller (BET) and using a surface area analyzer (metrometrics ASAP 2010). AgNPs were analyzed using transmission electron microscopy (TEM), which used a focused fine beam of electromagnetic lenses to generate high-resolution images.

RESULTS

Quantitative and Qualitative Analysis of Phytochemicals

Fig. (1) presents the qualitative and quantitative analysis of phenolic acids from HPLC-analyzed five medicinal plants. Different concentrations of Epicatechin, cinnamic acid, benzoic acid, Chlorogenic acid, 4-O-Caffeoylquinic acid, quercetin, and Rutin were detected in all the tested plants. The highest concentration of Rutin was noted in *M. olifera* (1303.1 mg/100g) followed by *J. excels* (232.9 mg/100g). The concentrations of flavanols were notably higher as compared to other compounds (Table 2).

GC–MS revealed the peak area, molecular weight, and molecular formula of constituents from all five plants. The results depicted the presence of fifty-one components in *J. excels* methanol extract mainly including 4,14-Retro-retinol (11.86 %), Podocarp-7-en-3β-ol, 13β-methyl-13-vinyl-(10.93%), and 1R-α-Pinene (8.65%) whereas the chromatogram of *M. olifera* presented five peaks. These compounds mainly included Vitamin E (51.67 %), α-Thujene (23.26 %), β-Terpinen (21.84 %), 3-Methyl-apopinene (1.77 %), and β-Farnesene (1.46 %). *P. dulce* chromatogram demonstrated seven peaks, which indicated the presence of seven compounds mainly including β-Sitosterol (10.44%), and Vitamin E, (5.50 %). The methanolic extract of *E. globulus* contained forty-nine compounds. The main components included (-)-Spathulenol (17.21 %), Globulol (12.08 %), Limonene (9.30 %), Ledene oxide-(II), and Bicyclo[3.2.0]heptane-2,6-diol, 5-(2-hydroxyethyl)-3,3-dimethyl-6-vinyl-, (Z)- (8.53 % and 8.43 %) whereas the presence of remaining components was minor.

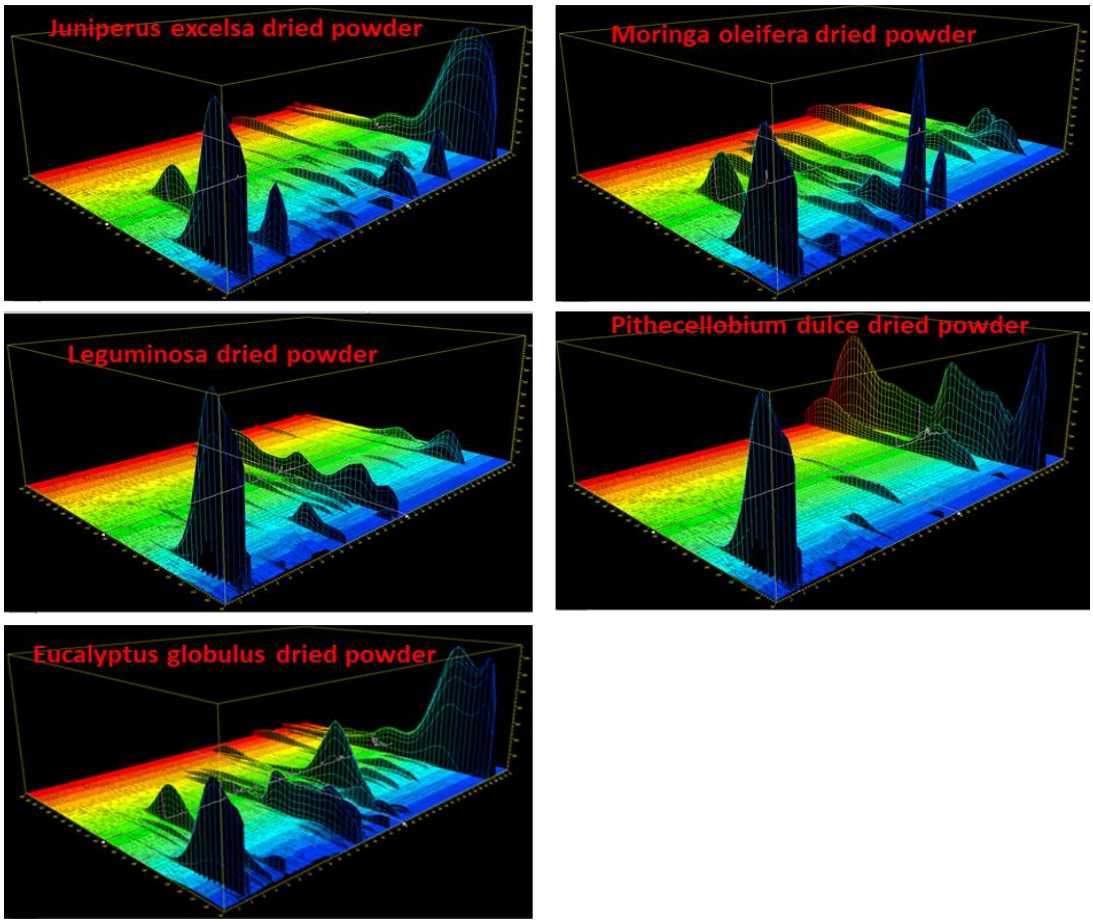

Fig. (1): 3D-DAD scan vs chromatogram of all samples that were SPE-analyzed after acid hydrolysis.

Table (2). Quantification of flavanols in Juniperus excels, Moringa oleifera, Prosopis juliflora, Pithecellobium dulce, and Eucalyptus globulus.

Sample→	S1	HS1	S2	HS2	S3	HS3	S4	HS4	S5	HS5
Compound↓	Flavanol content (mg/100g)									
EP	196.6	27.5	180.4	167.5	27.4	57.7	80.2	5.1	278.3	105.3
BE	74.9	5.2	0.0	0.0	32.6	4.9	0.0	5.1	84.3	60.1
CI	3.7	8.5	0.0	4.7	0.0	0.0	4.1	0.0	5.9	33.5
CH	8.6	9.2	16.0	3.6	8.6	4.1	11.4	4.4	338.3	159.5
CA	1.1	1.2	24.0	0.5	4.1	0.5	2.9	0.0	0.0	0.0
RU	232.9	117.4	1303.1	350.2	180.1	52.0	20.8	19.6	180.2	185.4
QU	5.7	111.4	0.0	512.3	8.7	6.1	0.0	906.5	9.2	312.2
SUM	**523.5**	**280.3**	**1523.4**	**1038.9**	**261.5**	**125.3**	**119.4**	**940.7**	**896.1**	**856.1**
GRAND TOTAL known and unknown flavonoids	**1309.0**	**862.4**	**3144.1**	**2047.7**	**1596.5**	**1120.3**	**3750.4**	**3982.8**	**1944.6**	**1875.2**

- Sample = S Hydrolyzed Sample = HS
- EP= epicatechin, BE= benzoic acid, CI=cinnamic acid, CH= chlorogenic acid, CA= 4-O-Caffeoylquinic acid, RU= rutin, QU= quercetin.
- S1= *J. excels*, S2= *M. oleifera*, S3= *P. juliflora*, S4= *P. dulce,* and S5= *E. globulus.*

Characterization of Silver Nanoparticles

The changed color (transparent to brown) of silver nitrate solution with plant extracts (*J. excels*, *M. oleifera*, *P. juliflora*, *P. dulce,* and *E. globulus*) represented the formation of plant extract capped silver nanoparticles (AgNps). UV-VIS spectrograph of silver nanoparticles' colloidal solution confirmed it as a function of time. Fig. (2) demonstrates the recorded UV-VIS spectra of the reaction medium after 24 hours. The absorption spectra (300 nm) of silver nanoparticles in reaction media confirmed the AgNPs formation whereas the broadening peak indicated that AgNPs were polydispersed.

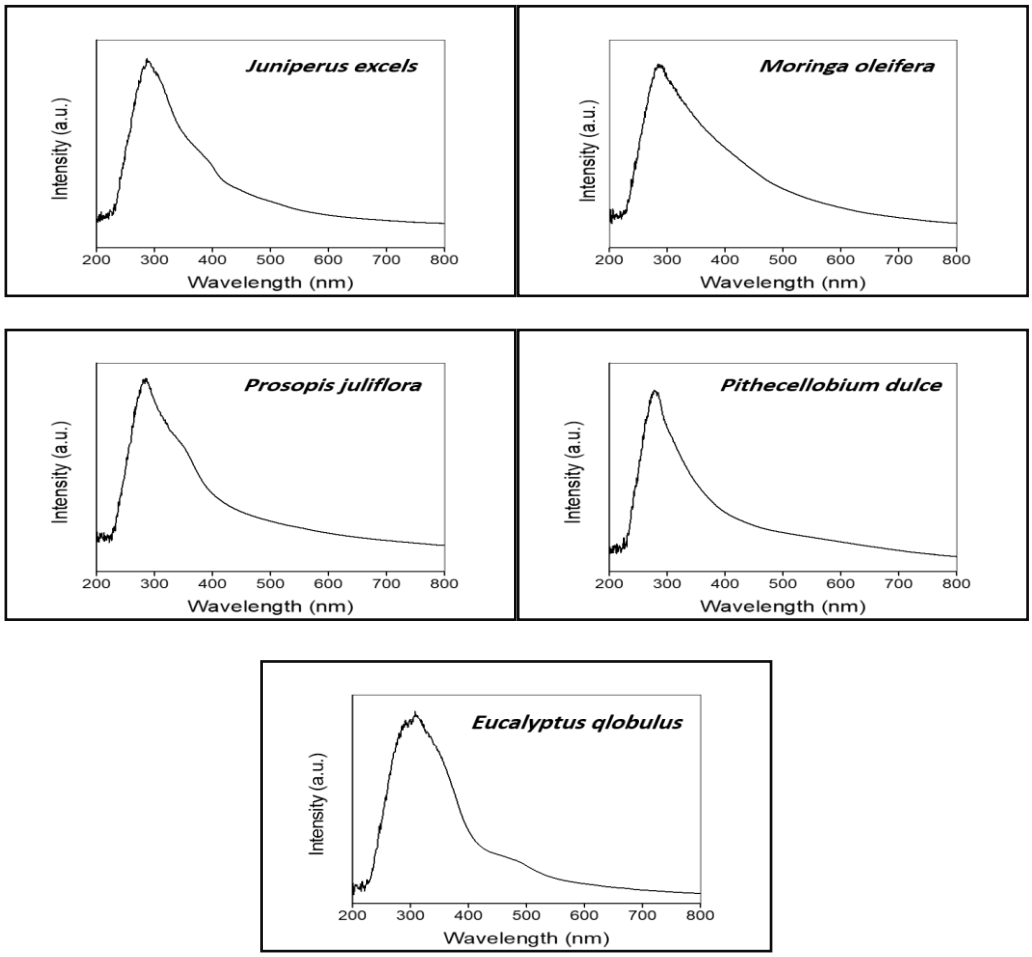

Fig. (2): UV–vis spectrum of green synthesized AgNPs using plant extracts.

XRD was used to investigate the crystalline nature of green synthesized AgNPs (Fig. 3). Three major peaks were observed at 38.1, 45, 65, and 78°C corresponding to 111, 200, 142, 220, and 311 planes of crystalline structures in silver, respectively. The minor peaks in the XRD pattern might be due to bio-organic phase crystallization in culture extract. A peak at 31.9 represented the existence of Ag2O [14]. FT-IR analysis (Fig. 4) revealed an intense and broad absorption band between 3500 and 3400 cm^{-1} with tested plant extracts and a medium peak was noted at 1650 cm^{-1}. Mariselvam et al. (2014) have reported an FT-IR analysis-based absorption band at 1638 cm^{-1}, which established the bio moieties capped AgNPs formation [15]. Transmission electron microscopy images of AgNPs formation with *P. juliflora* and *E. gobulus* are presented

in Figures (5) and (6). The particles had a spherical shape within a narrow range of particle size (5 to 20 nm), and the average size was calculated as 8.7 nm. *P. juliflora* and *E. gobulus* AgNPs were well dispersed without any agglomeration.

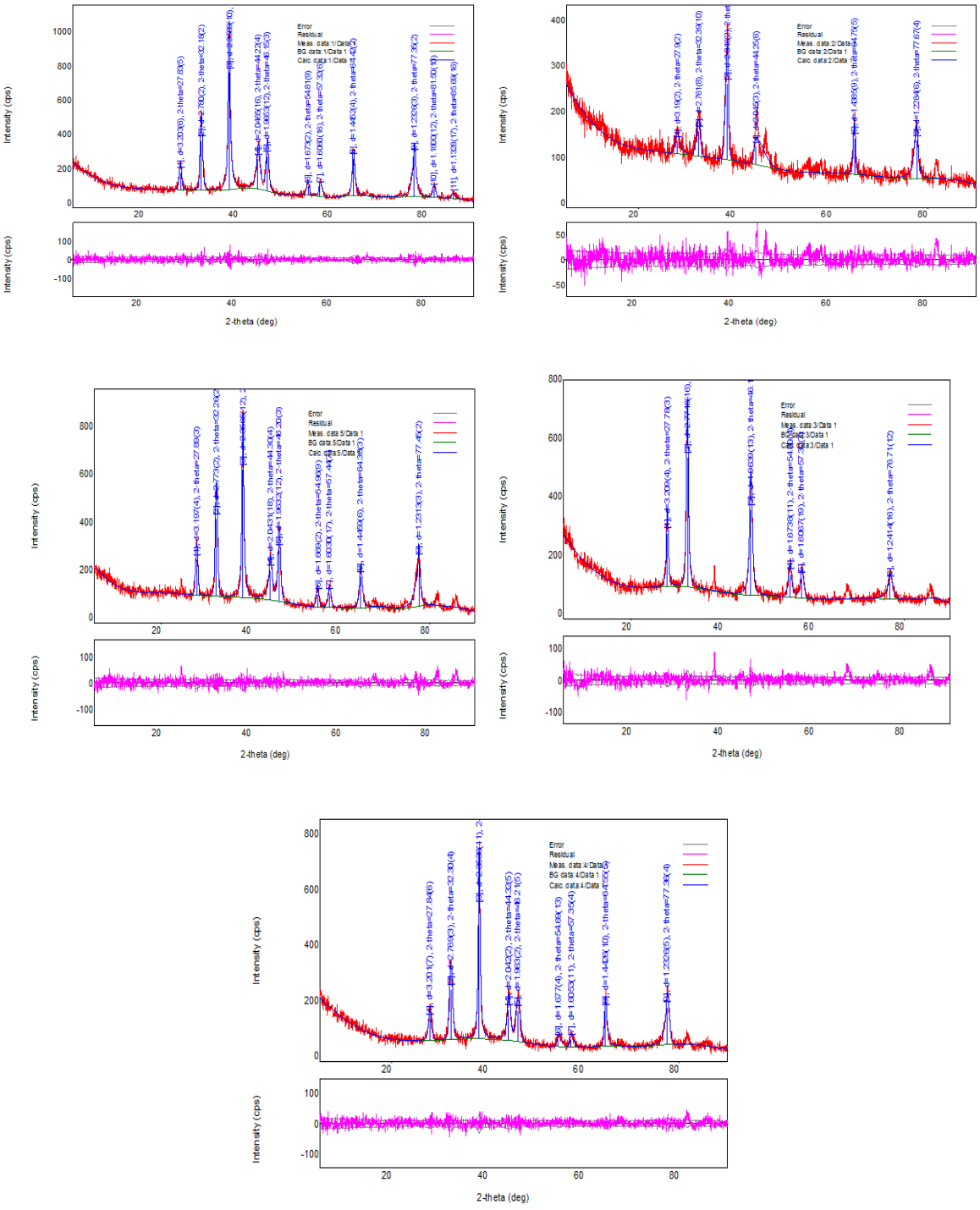

Figs. (3): XRD spectra of biosynthesized AgNPs.

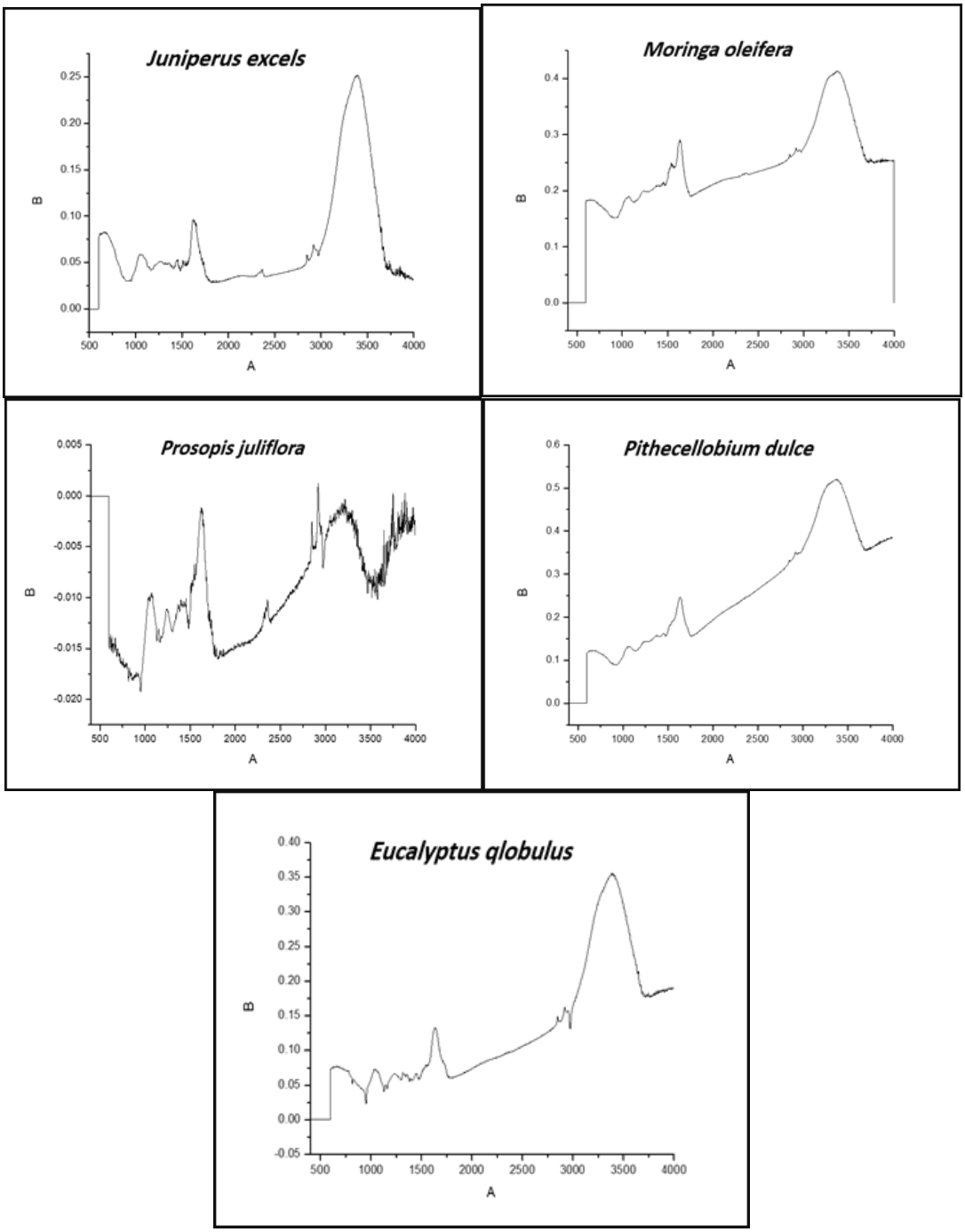

Fig. (4): FT-IR analysis of green synthesized AgNPs.

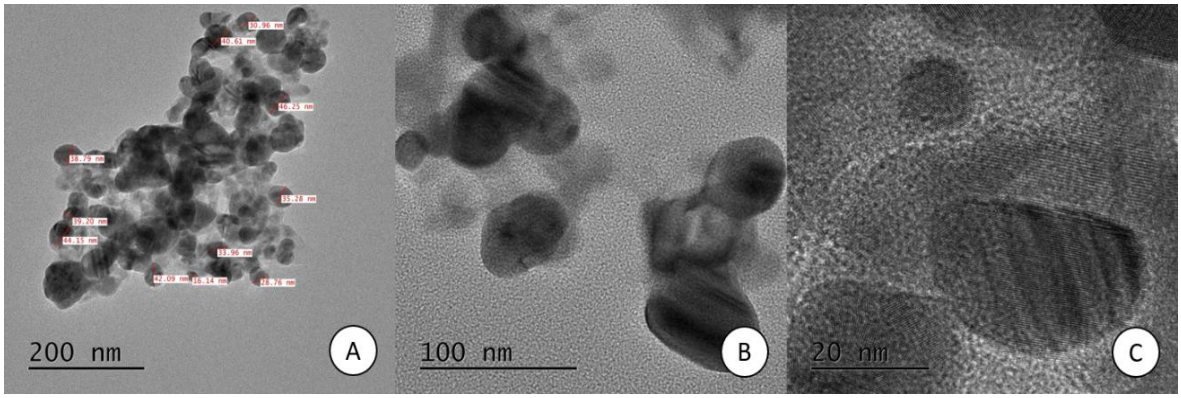

Fig. (5): Transmission electron microscopy of AgNPs biosynthesized using *P. juliflora* leaf extract (A=200 nm, B=100 nm, and C= 20 nm).

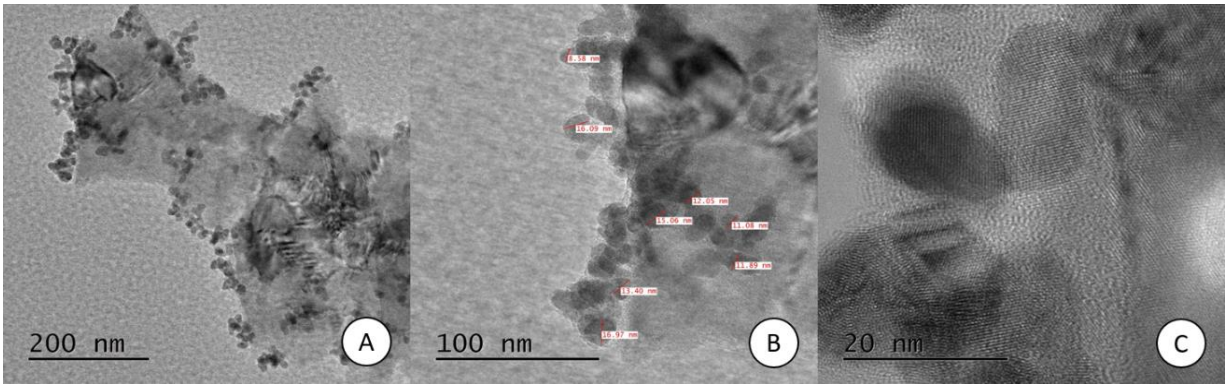

Fig. (6): Transmission electron microscopy of AgNPs biosynthesized using *E. globulus* leaf extract (A=200 nm, B=100 nm, and C= 20 nm).

DISCUSSION

Surface plasmon vibrations (SPR) generated the specific color of the synthesized silver nanoparticles. The qualitative assessment of reduction potential revealed that all the tested plant extracts contained a significant amount of reducing entities. Silver nitrate reduction to silver element during fungi and bacteria-mediated AgNP synthesis is associated with the activity of reductive enzymes [8]. However, plant extract components-based silver nitrate reduction to silver element is debatable. The involvement of theophylline and caffeine-based reduction has also been reported during the synthesis of silver nanoparticles. UV-Vis spectrograph of AgNPs colloidal solution was recorded as a function of time. Fig. (2) demonstrates the UV-Vis spectra of the reaction medium after 24 hours of treatment. AgNPs absorption peak with tested plant extracts was noted at 300 nm, which is in agreement with the findings of Ameen *et al*. (2019) [16]. UV-Vis spectroscopy further confirmed the nanoscale and plasmon resonance of the silver surface. Multiple studies have reported the plant leaf extract-based absorbance peak within a range of 300-500 nm [16]. The flavonoids in the plant leaf extracts (aqueous) played a critical role in $AgNO_3$ reduction to synthesize AgNPs. Sathishkumar *et al*. (2016 a,b) have reported the capping and reduction capabilities of carbonyl and hydroxyl groups of flavonoids in reducing X-ray diffraction analysis established the crystalline structure of green AgNPs synthesized with five plant extracts [8, 12]. Four major peaks were observed at 38.1, 45, 65, and 78°C corresponding to 111, 200, 142, 220, and 311

planes of silver crystalline structures. The emergence of minor peaks in the XRD pattern could be attributed to the crystallization of the bio-organic phase of plant extracts. The peak at 31.9 represented the existence of Ag_2O [14]. Fourier transform infrared spectroscopy (FT-IR) detected the presence of functional groups in the biomolecules of plant extracts. FT-IR analysis depicted an intense and broad absorption band between 3500 and 3400 cm^{-1} with the tested plant leaf extracts. *P. juliflora* extract presented a medium peak at 1650 cm^{-1}. Mariselvam *et al*. (2014) have also reported an FT-IR analysis-based absorption band at 1638 cm^{-1}, which indicated the bio moieties-capped AgNPs formation [15].

Transmission electron microscopy (TEM) is a powerful tool to investigate the chemistry and structure of different materials including nanoparticles of size below 100 nm [17, 18]. TEM images were used to determine the NPs size distribution and matched it with the XRD-based calculation of average particle size. Different shape models (oval, sphere, and square) were applied to measure the particle size. TEM can efficiently image the plant nanomaterials (single atoms to small-size NPs), however, a suitable electron beam should be used to image the materials with 5 nm or smaller size [18]. Several studies have employed TEM to investigate the size and shape of nanoparticles [19, 20]. TEM imaging revealed an average nanoparticle size of 8.7 nm. *P. juliflora* and *E. gobulus* NPs were well dispersed without any agglomeration. TEM analysis revealed only minor particle-to-particle adherence without any Extract-NPs fusion that could be associated with the corona formation by *P. juliflora* and *E. gobulus* extract biomolecules during NPs capping [21]. Figures 5-6 reveal the lattice d-spacing of 0.226 nm and distance between planes. This ¬d-spacing confirmed the crystallinity of extract-capped AgNPs. Unla *et al*. (2008) and Küçük *et al*. (2016) have studied the efficiency of *J. excelsa* Bieb. subsp. *excelsa* extract against *Candida krusei* (ATCC® 6258) and *C. parapsilosis* (ATCC® 22019), which led to moderate *Candida* activity [22]. The effects of *J. excelsa* and its individual constituents' interaction on antimicrobial activity are not fully understood. However, *J. excelsa* leaves essential oil is known to contain a high percentage of limonene [23, 24]. Similarly, a predominant presence of α-pinene (22.5%, 29.7%, 32.34%, and 8.65 (5.01-14.04%)) has been reported in *J. excels* leaves essential oil samples from different countries (Greece, Turkey, and Iran) [25].

Phytochemicals (isothiocyanates or flavonoids) significantly contribute to the *M. oleifera* plant extract's bioactivity [26]. Oladeji *et al*. (2019) have thoroughly screened the phytochemical composition of *M. oleifera* leaf extracts and reported the presence of important bioactive compounds including phlorotannins, steroids, terpenoids, saponins, flavonoids, and tannins [27]. During this study, the presence of Vitamin E in *M. oleifera* leaves extract was noted to be comparable with the previous report of Moyo *et al*. (2011) [28]. Aja *et al*. (2015) have reported the presence of L-(+)-Ascorbic acid 2,6-dihexadecanoate (19.66%), 9-Otadecenoic acid (20.89%), and other components in *M. oleifera* leaves whereas other studies have demonstrated the presence of flavones (Rutin, Chlorogenic acid, and Epicatechin) in *M. olifera* [29-32]. Leone *et al*. (2015) have stated that high inter-studies variations of these compounds could be due to varying harvesting seasons, environmental conditions, plant genetics, dry method, stage of leaf maturity, extraction methods, and sensitivity of the applied analytical techniques [33]. *P. juliflora* plant contained high amounts of benzoic acid, rutin, quercetin, and chlorogenic acid. Ukande *et al.* (2019) have reported the presence of several alkaloids in *P.*

juliflora and studied their antimicrobial potential against Gram-negative (*E. coli*) and Gram-positive (*S. aurus*) bacteria and fungi [34]. Different investigations have also reported high amounts of phenolic compounds and flavonoids in *P. juliflora* [35, 36].

significant amounts of flavonols including rutin, benzoic acid, cinnamic acid, and chlorogenic acid [37]. Different plant parts mainly contained 38 active phyto-compounds such as dulcitol, quercetin, and kaempferol. High secondary metabolite (saponin, flavonoid,) concentrations demonstrated inhibitory effects against fungal and bacterial growth [38-40]. Aldoghaim *et al*., (2018) performed antimicrobial and phytochemical analyses of *E. globulus* leaves [41]. The data depicted high percentages of p-cymene and limonene. Kassahun and Feleke (2019) have reported the presence of α-pinen, epiglobulol, p-Cymene, aromadendrene, ledol, and globulol in *E. globulus* leaves [42]. Mekonnen *et al* (2015) have also found limonene and α-Pinen in *E. globulus* leaves [43]. Pan, *et al.* (2019) have reported eucalyptol (21.49%) as the main compound of *E. globulus* whereas quercetin, benzoic acid, and chlorogenic acid have been reported as well [44].

CONCLUSION

The significantly varying antimicrobial properties of plant extracts could be attributed to differential phytochemicals. Therefore, plant extracts were screened for phytochemical constituents using HPLC and GC-MS techniques during this study. The anti-microbial activity of these extracts could be associated with the presence of phytochemicals. A “green” method was successfully employed for AgNP synthesis, which was further confirmed through UV, XRD, FTIRs, and TEM analyses. The results confirmed the antimicrobial features of tested plant extracts and they could be potentially employed to treat infectious diseases.

ACKNOWLEDGMENT

The authors thankfully acknowledge the technical and financial support of the University of Jeddah.

References

1. Ochola, S.O., et al., *Antifungal activity of methanol extracts of Leonotis nepetifolia L. and Ocimum gratissimum L. against Ascochyta blight (Phoma exigua) on French bean.* Asian Journal of Plant Pathology, 2015. 9(1): p. 27-32.

2. Kirbag, S., F. Zengin, and M. Kursat, *Antimicrobial activities of extracts of some plants.* Pak. J. Bot, 2009. 41(4): p. 2067-2070.

3. Madhuri, S. and G. Pandey, *Some anticancer medicinal plants of foreign origin.* Current science, 2009: p. 779-783.

4. Nascimento, G.G.F., et al., *Antibacterial activity of plant extracts and phytochemicals on antibiotic-resistant bacteria.* Brazilian journal of microbiology, 2000. 31: p. 247-256.

5. Zumla, A., et al., *The WHO global tuberculosis report "further to go.* The Lancet Global Health, 2015. 3(1): p. e10-e12.

6. Sun, J., Z. Deng, and A. Yan, *Bacterial multidrug efflux pumps: mechanisms, physiology and pharmacological exploitations.* Biochemical and biophysical research communications, 2014. 453(2): p. 254-267.

7. Allahverdiyev, A.M., et al., *Coping with antibiotic resistance: combining nanoparticles with antibiotics and other antimicrobial agents.* Expert review of anti-infective therapy, 2011. 9(11): p. 1035-1052.

8. Sathishkumar, P., et al., *Anti-acne, anti-dandruff and anti-breast cancer efficacy of green synthesised silver nanoparticles using Coriandrum sativum leaf extract.* Journal of Photochemistry and Photobiology B: Biology, 2016a. 163: p. 69-76.

9. Parlinska-Wojtan, M., et al., *Green synthesis and antibacterial effects of aqueous colloidal solutions of silver nanoparticles using camomile terpenoids as a combined reducing and capping agent.* Bioprocess and biosystems engineering, 2016. 39: p. 1213-1223.

10. Jadhav, K., et al., *Green and ecofriendly synthesis of silver nanoparticles: characterization, biocompatibility studies and gel formulation for treatment of infections in burns.* Journal of Photochemistry and Photobiology B: Biology. 155: p. 109-115.

11. Inbathamizh, L., T.M. Ponnu, and E.J. Mary, *In vitro evaluation of antioxidant and anticancer potential of Morinda pubescens synthesized silver nanoparticles.* Journal of Pharmacy Research, 2013. 6(1): p. 32-38.

12. Sathishkumar, P., et al., *Phyto-synthesis of silver nanoparticles using Alternanthera tenella leaf extract: An effective inhibitor for the migration of human breast adenocarcinoma (MCF-7) cells.* Bioprocess and biosystems engineering, 2016b. 39: p. 651-659.

13. Sreelatha, S. and P.R. Padma, *Antioxidant activity and total phenolic content of Moringa oleifera leaves in two stages of maturity.* Plant foods for human nutrition, 2009. 64: p. 303-311.

14. Liu, X., et al., *XRD investigation of ion irradiated Ti3Si0. 90Al0. 10C2.* Nuclear Instruments and Methods in Physics Research Section B: Beam Interactions with Materials and Atoms, 2010. 268(5): p. 506-512.

15. Mariselvam, R., et al., *Green synthesis of silver nanoparticles from the extract of the inflorescence of Cocos nucifera (Family: Arecaceae) for enhanced antibacterial activity.* Spectrochimica Acta Part A: Molecular and Biomolecular Spectroscopy, 2014. 129: p. 537-541.

16. Ameen, F., et al., *Prevalence of antibiotic resistant mastitis pathogens in dairy cows in Egypt and potential biological control agents produced from plant endophytic actinobacteria.* Saudi journal of biological sciences, 2019. 26(7): p. 1492-1498.

17. Su, B., Q. Guan, and S. Yu, *The neurotoxicity of nanoparticles: a bibliometric analysis.* Toxicology and Industrial Health, 2018. 34(12): p. 922-929.

18. Anjum, D.H. *Characterization of nanomaterials with transmission electron microscopy*. in *IOP Conference Series: Materials Science and Engineering*. 2016. IOP Publishing.

19. Behravan, M., et al., *Facile green synthesis of silver nanoparticles using Berberis vulgaris leaf and root aqueous extract and its antibacterial activity.* International journal of biological macromolecules, 2019. 124: p. 148-154.

20. Mmola, M., et al., *Enhanced antimicrobial and anticancer activity of silver and gold nanoparticles synthesised using Sargassum incisifolium aqueous extracts.* Molecules, 2016. 21(12): p. 1633.

21. Ameen, F., et al., *Soil bacteria Cupriavidus sp. mediates the extracellular synthesis of antibacterial silver nanoparticles.* Journal of Molecular Structure, 2020. 1202: p. 127233.

22. Unlu, M., et al., *Composition and antimicrobial activity of Juniperus excelsa essential oil.* Chemistry of Natural Compounds, 2008. 44: p. 129-131.

23. Kakar, H., et al., *Chemical composition, antimicrobial and antileishmanial activity of essential oil of Juniperus excelsa M. Bieb. from Ziarat, Balochistan.* Pure and Applied Biology (PAB), 2017. 6(3): p. 786-796.

24. Khoury, M., et al., *Chemical composition and antimicrobial activity of the essential oil of Juniperus excelsa M. Bieb. growing wild in Lebanon.* Chemistry & biodiversity, 2014. 11(5): p. 825-830.

25. Asili, J., et al., *Chemical and antimicrobial studies of Juniperus excelsa subsp. excelsa and Juniperus excelsa subsp. polycarpos essential oils.* Journal of Essential Oil Bearing Plants, 2008. 11(3): p. 292-302.

26. Kou, X., et al., *Nutraceutical or pharmacological potential of Moringa oleifera Lam.* Nutrients, 2018. 10(3): p. 343.

27. Oladeji, O.S., K.A. Odelade, and J.K. Oloke, *Phytochemical screening and antimicrobial investigation of Moringa oleifera leaf extracts.* African Journal of Science, Technology, Innovation and Development, 2019. 12(1): p. 79-84.

28. Moyo, B., et al., *Nutritional characterization of Moringa (Moringa oleifera Lam.) leaves.* African Journal of Biotechnology, 2011. 10(60): p. 12925-12933.

29. Aja, P.M., et al., *Evaluation of anti-diabetic effect and liver function indices of ethanol extracts of Moringa oleifera and Cajanus cajan leaves in alloxan induced diabetic albino rats.* Global Veterinaria, 2015. 14(3): p. 439-447.

30. Coppin, J.P., et al., *Determination of flavonoids by LC/MS and anti-inflammatory activity in Moringa oleifera.* Journal of Functional Foods, 2013. 5(4): p. 1892-1899.

31. Zhang, M., et al., *Phytochemicals, antioxidant and antimicrobial activity of Hibiscus sabdariffa, Centella asiatica, Moringa oleifera and Murraya koenigii leaves.* J. Med. Plants Res, 2011. 5(30): p. 6672-80.

32. Singh, B.N., et al., *Oxidative DNA damage protective activity, antioxidant and anti-quorum sensing potentials of Moringa oleifera.* Food and chemical toxicology, 2009. 47(6): p. 1109-1116.

33. Leone, A., et al., *Cultivation, genetic, ethnopharmacology, phytochemistry and pharmacology of Moringa oleifera leaves: An overview.* International journal of molecular sciences, 2015. 16(6): p. 12791-12835.

34. Ukande, M.D., et al., *Review on Pharmacological potentials of Prosopis juliflora.* Journal of Drug Delivery and Therapeutics, 2019. 9(4-s): p. 755-760.

35. Rechab, S.O., et al., *Antioxidant activity and antimicrobial properties of Entada leptostachya and Prosopis juliflora extracts.* Journal of Medicinal Plants for Economic Development, 2018. 2(1): p. 1-8.

36. Malik, S.K., M. Ahmed, and F. Khan, *Identification of novel anticancer terpenoids from Prosopis juliflora (Sw) DC (Leguminosae) pods.* Tropical Journal of Pharmaceutical Research, 2018. 17(4): p. 661-668.

37. Murugesan, S., et al., *Nutritional and therapeutic benefits of medicinal plant Pithecellobium dulce (Fabaceae): A review.* Journal of Applied Pharmaceutical Science, 2019. 9(7): p. 130-139.

38. Sukantha, T.A., S.K. Sripathi, and N.T. Ravindran, *Antibacterial activity of selected medicinal plant in traditional treatment of wound infection in Southeast India.* International Journal of Pharmacy and Pharmaceutical Sciences, 2014: p. 511-513.

39. Shanmugakumar, S.D., S. Amerjothy, and K. Balakrishna, *Pharmacognostical, antibacterial and antifungal potentials of the leaf extracts of Pithecellobium dulce Benth.* Pharmacognosy Magazine, 2006. 2(7): p. 163-167.

40. Bautista-Ba¡±os, S., et al., *Seasonal evaluation of the postharvest fungicidal activity of powders and extracts of huamuchil (Pithecellobium dulce): action against Botrytris cinerea, Penicillium digitatum and Rhizopus stolonifer of strawberry fruit.* Postharvest biology and technology, 2003. 29(1): p. 81-92.

41. Aldoghaim, F.S., G.R. Flematti, and K.A. Hammer, *Antimicrobial activity of several cineole-rich Western Australian Eucalyptus essential oils.* Microorganisms, 2018. 6(4): p. 122.

42. Kassahun, A. and G. Feleke, *Chemical composition and physico-chemical analysis of Eucalyptus globulus leave and oil.* Science Journal of Chemistry, 2019. 7(2): p. 36-38.

43. Mekonnen, A., et al., *In vitro antimicrobial activity of essential oil of Thymus schimperi, Matricaria chamomilla, Eucalyptus globulus, and Rosmarinus officinalis.* International journal of microbiology, 2015. 2016.

44. Pan, M., et al., *A strategy based on GC-MS/MS, UPLC-MS/MS and virtual molecular docking for analysis and prediction of bioactive compounds in Eucalyptus globulus leaves.* International journal of molecular sciences, 2019. 20(16): p. 3875.